Title
CHEMICAL AND OPTICAL PROPERTIES OF ELECTPOCHROMIC NICKEL OXIDE FILMS

Authors
Lampert, CM.
Omstead, T.R.
Yu, P.C.

Publication Date
1985-08-01

Lawrence Berkeley Laboratory

UNIVERSITY OF CALIFORNIA

APPLIED SCIENCE DIVISION

Presented at the SPIE 29th Annual International Technical Symposium on Optical and Electro-Optical Engineering, San Diego, CA, August 18-23, 1985

CHEMICAL AND OPTICAL PROPERTIES OF ELECTROCHROMIC NICKEL OXIDE FILMS

C.M. Lampert, T.R. Omstead, and P.C. Yu

August 1985

APPLIED SCIENCE DIVISION

Prepared for the U.S. Department of Energy under Contract DE-AC03-76SF00098

DISCLAIMER

LBL-20211
EEB-W 85-13
W/OM-202

Presented at the SPIE's 29th Annual International Technical Symposium on Optical and Electro-Optical Engineering, San Diego, CA, 18-23 August, 1985.

CHEMICAL AND OPTICAL PROPERTIES OF ELECTROCHROMIC NICKEL OXIDE FILMS

C. M. Lampert, T.R. Omstead, and P.C. Yu

Applied Science Division
and
Materials and Molecular Research Division
Lawrence Berkeley Laboratory
University of California
Berkeley, California 94720

August 1985

This work was supported by the Assistant Secretary for Conservation and Renewable Energy, Office of Building Energy Research and Development, Building Systems Division of the U.S. Department of Energy under Contract No. DE-ACO3-76SF00098.

Chemical and Optical Properties of Electrochromic Nickel Oxide Films

C. M. Lampert, T.R. Omstead*, P. C. Yu

Applied Science Division and Materials and Molecular Research Division,
Lawrence Berkeley Laboratory, University of California, Berkeley, Calif. 94720 U.S.A.

Abstract

Thin films of nickel oxide-nickel hydroxide are investigated to determine electrochromic switching properties. Crystalline nickel oxide films are synthesized by electrochemical deposition and by anodization of nickel electrodes. Electrochemical deposition using nickel sulfate-based chemistry is used to deposit films directly on doped tin oxide-coated glass. Spectral solar transmittance is obtained for films switched in liquid cells containing a KOH electrolyte. The solar transmittance (T_s) can be switched from T_s (bleached) = 0.73 to T_s (colored)= 0.35 for films with thickness of about 500 A. Voltammetric data is correlated to known electrochemical processes for nickel electrodes. The nickel oxide films are chemically analyzed using a sputter-Auger microprobe and x-ray photoelectron spectroscopy. As a result of combined analysis, it was determined that these films transform from uncolored to colored states by the reversible transformation of nickel hydroxide $Ni(OH)_2$ to nickel oxyhydroxide NiOOH and that dehydrated films correspond chemically to NiO.

Introduction

The property of electrochromism is very important to the development of large-area optical shutters and information displays, where switching speed is not a key consideration. From a building energy efficiency viewpoint in regard to glazings, the ability to dynamically control the incoming solar radiation either in the visible or near-infrared spectral regions is very attractive. Also, electrochromism has importance to future automotive and aerospace glazings.

Electrochromism is known to occur in several transition-metal oxides. A few reviews on the subject detail the outcome of different investigations (1-4). Chiefly, tungsten oxide (WO_3) and hydrated iridium oxide ($IrO_x \cdot nH_2O$) have been studied in some detail. As for the other oxides, such as $NiOO_x \cdot nH_2O$ and $MnO_x \cdot nH_2O$, very little is known about their electrochromic properties (5).

The characteristics of electrochromism are manifested by a reversible color change, usually switching from an uncolored state to a colored one, as a result of an applied electric current. Electrochromic materials exhibit both chemical and optical changes by dual ion and electron ejection or injection. As a result, color centers are formed in the material that produce optical adsorption in the visible wavelength region. Also, in certain cases, large changes in electrical conductivity can occur causing significant infrared reflectivity switching effects (6). Coloration of an electrochromic material can occur on either the cathodic or anodic cycle. For nickel oxide, coloration occurs by chemical oxidation during anodization. A very important property of electrochromic films is that they exhibit mixed conductivity, both electronic and ionic, in which ions can be rapidly and reversibly inserted in step with injected or ejected electrons (7).

As a matter of example, it is important to detail the switching effect of the electrochromic layer in an actual solid-state device structure. Shown in Figure 1 is the cross section of a typical solid-state device. Although other configurations exist, including liquid electrolytes in place of the ion conductor, this example serves to demonstrate the device complexity. In this five-layer model there is symmetry about the ion conductor. Both the electrochromic layer and counter-electrode (ion storage media) exhibit mixed ionic and electronic conduction. These layers are flanked by transparent conductors (SnO_2:F, Cl or In_2O_3:Sn), which serve as electrical conductors. The ionic conductor provides a medium by which ions can be transported between the electrochromic layer to the counter-electrode depending upon the polarity of the applied potential. As a result, a reversible ionic reaction between the electrochromic material and counter-electrode allows for the appropriate optical switching effect. Before the development of such a device, it is important to fully characterize the electrochemical and optical properties of the electrochromic material. In the following experiments, nickel oxide film properties are determined by techniques of voltammetry, sputter Auger spectroscopy, x-ray photoelectron spectroscopy (XPS, ESCA), and optical spectrophotometry.

*Currently with Univ. of Minnesota, Dept. of Chemical Engineering and Material Science, Minneapolis, MN. 55455.

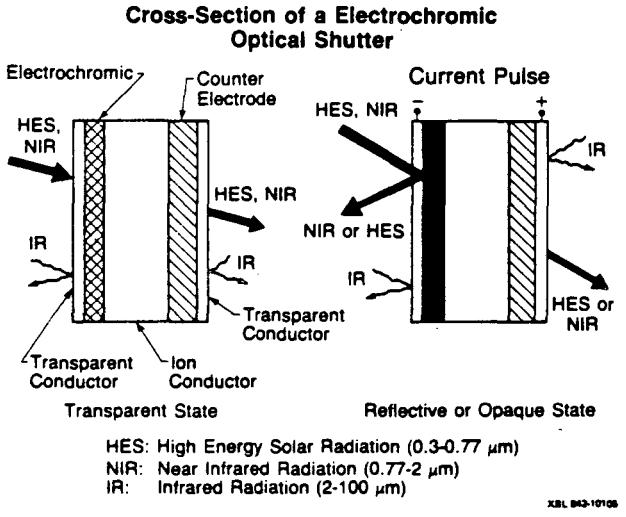

Figure 1. Schematic cross section of an electrochromic optical shutter.

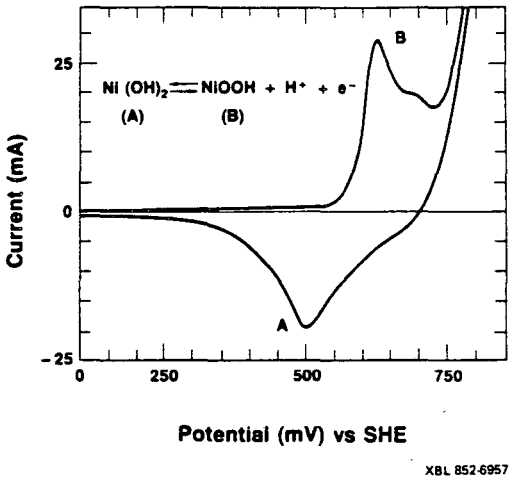

Figure 2. Cyclic voltammetry of NiO/ Ni electrode in 1M KOH solution after twelve cycles.

Experimental Procedures

In this study both metallic nickel electrodes and transparent conductive oxide-coated glass electrodes were used. The metal electrode was made from a 1.59-mm nickel plate (0.999 pure). It was polished with silicon carbide paper (in sequence from 180-600 grits) followed by 6-micron diamond paste and finished by a series of alumina abrasives (in sequence from 1 to 0.3 to 0.05 microns). Distilled water was used as a lubricant for polishing. To provide electrical contact, a nickel wire was spot welded on to the back of the electrode.

By using a scanning potentiostat, Princeton Applied Research Model 362, a controlled wavefunction was applied to the electrode. Electrooxidation was achieved by using a sawtooth wavefunction alternating between -800 mV and +1800 mV in a 1M KOH electrolyte. The wavefunction was monitored by an oscilloscope, and the voltage was monitored by a multimeter. After several hours of cyclic oxidation of the electrode, visible optical switching was observed on the surface. The observed coloration was from transparent (metallic) to bronze. Also, it was observed that the electrode, when removed from the bath, could last a few hours in the colored state with negligible fading.

The second group of experiments was done on fluorine doped tin oxide-coated glass. The tin oxide (SnO_2: F, Cl) coating was produced by conventional chemical vapor deposition, involving hydrolysis of $SnCl_4$ and NH_4F (8). This coating had a sheet resistance of 110 Ω/sq., and a copper wire was attached to the conductive coating with silver epoxy.

The electrochemical working solution used to deposit the nickel oxide was a mixture of 0.1M $NiSO_4 \cdot 6H_2O$ and 0.1M NH_4OH at 23°C. A platinum electrode served as the counter-electrode. The applied potential was a sawtooth wavefunction from -275 mV to +750 mV at 0.1 Hz frequency. The nickel hydroxide film formed after three cycles. After rinsing in distilled water, the electrode was transferred to another electrolyte of 1M KOH. In this bath electrochromic switching occured after at least twelve cycles at +200 mV to +900 mV (SHE). Depending upon the exact conditions of deposition, the electrode could remain out of solution in its colored state for several hours before fading. The electrode color ranged from transparent to dark bronze.

Other bath compositions were experimented with before the former was developed. A bath consisting of 0.1M $NiSO_4 \cdot 6H_2O$, 0.1M NaAc, and 0.001M KOH under the same conditions made acceptable films but provided less uniformity in the deposit. Another bath consisted of 0.45M $Ni(NO_3) \cdot 6H_2O$, and 1.75M NaOH. It provided good uniformity but lesser stability than the sulfate baths.

Spectral transmittance measurements were made to investigate the optical response of the films. Spectral data were obtained on a Perkin Elmer Lambda 9 spectrophotometer from 200-3200 nm.

The chemical composition of the conductive electrode was analyzed with the Scanning Auger Microprobe, Physical Electronics Inc., Model 590. A primary beam energy of 5 keV was used. Chemical depth profiles were obtained by using an argon sputter ion beam insitu in the vacuum chamber. The sputter etch rate was calibrated to 1000 A/min in Ta_2O_5.

X-ray photoelectron spectroscopy (Physical Electronics Inc., Model 548) was used to analyze the chemical states of the various elemental species. The spectrometer was calibrated so that the gold $4F_{7/2}$ electron binding energy was at 83.8 eV, and adventitious carbon occured at 284.4 eV ± 0.1 eV. Magnesium x-ray radiation at 400 W was used as the excitation radiation.

Results and Discussion

This section is divided into two major parts. The first part concerns results on the nickel electrode. The second portion details studies on the nickel oxide/tin oxide/glass electrode.

Nickel Electrode Study

Electrochemical information was obtained by cyclic voltammetry of the electrooxidized nickel electrode. The scanning potentiostat was used with a triangle potential from 0-800 mV (SHE) at 23°C The cell was IR compensated, and the 1M KOH electrolyte was purified of oxygen by nitrogen gas saturation. In Figure 2, the results of this experiment are shown for sweep characteristics of 20 mV/sec after twelve cycles. The anodic peak (B) at 625 mV corresponds to $Ni(OH)_2$ $NiOOH + H^+ + e^-$, and the cathodic peak (A) at 500 mV corresponds to $NiOOH + H^+ + e^- \longrightarrow Ni(OH)_2$. These reactions have been observed by various authors (9-14). The electrooxidation sequence begins with nickel metal (Ni), which is electrooxidized by an anodic potential occurring at +500 mV (SHE) resulting in the formation of NiO or $Ni(OH)_2$ During this process the nickel surface has been transformed from Ni--> Ni(II). In the voltammogram shown in Figure 2, the first anodic peak (B) corresponds to electrooxidation of Ni(II)--> Ni(III), forming a nickel oxyhydroxide phase such as β-NiOOH. The next anodic peak corresponds to oxygen evolution (750- 775 mV). For the cathodic cycle, electroreduction of Ni(III) yields Ni(II), identified as NiO or $Ni(OH)_2$ These compounds can be further electroreduced to nickel only at high cathodic potentials.

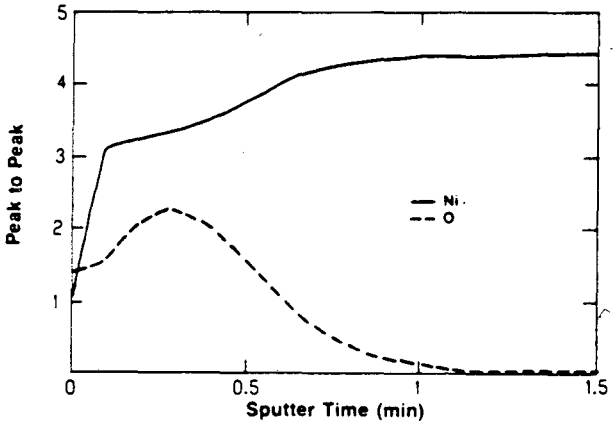

Figure 3. Auger sputter depth profile of NiO/ Ni of its peak to peak intensities showing nickel and oxygen as a function of depth from the surface (sputter rate is 1000 A/min for Ta_2O_5).

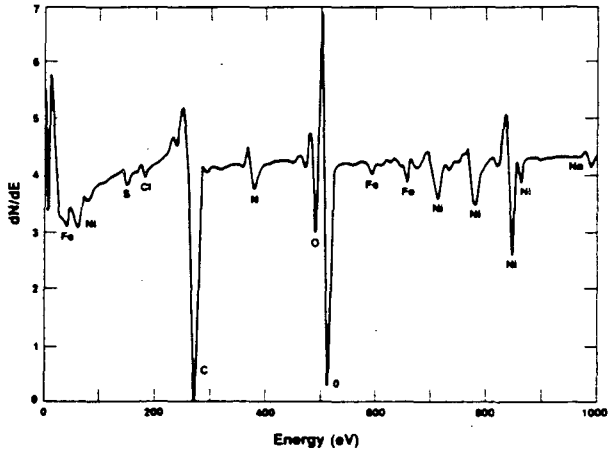

Figure 4a. Auger electron spectroscopy of NiO/ Ni electrode, as received.

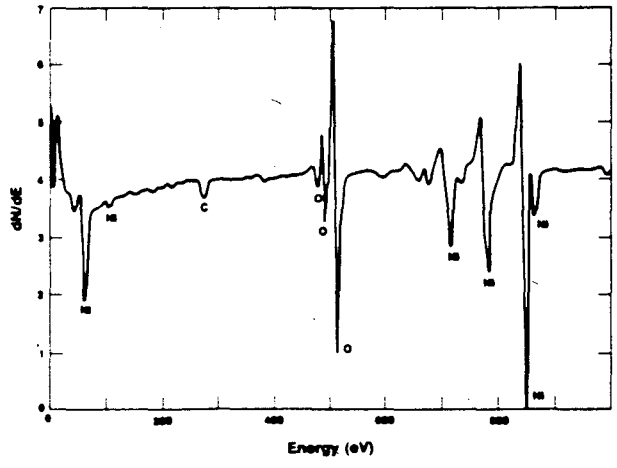

Figure 4b. Auger electron spectroscopy of NiO/ Ni after 15 seconds of argon-ion sputtering.

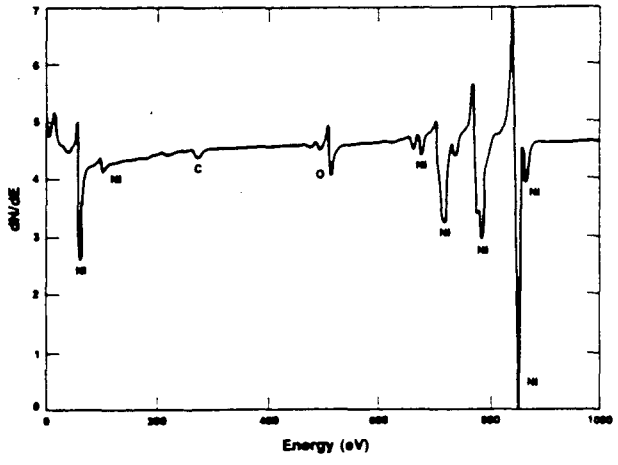

Figure 4c. Auger electron spectroscopy of NiO/ Ni after 60 seconds of argon-ion sputtering.

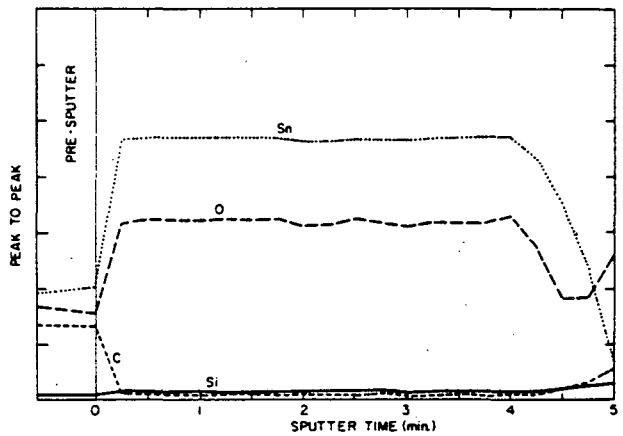

Figure 5a. Auger sputter depth profile of SnO_2:F, Cl/glass electrode of its peak to peak intensities showing uniformity in composition (sputter rate is 400 Å/min for Ta_2O_5).

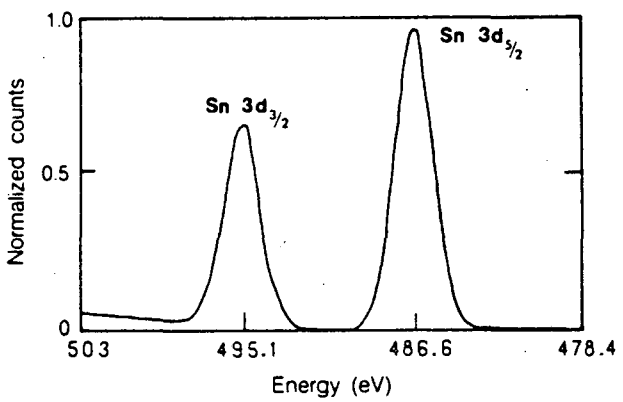

Figure 5c. X-ray photoelectron spectroscopy of tin 3d electrons in SnO_2:F, Cl, showing the characteristic binding energies.

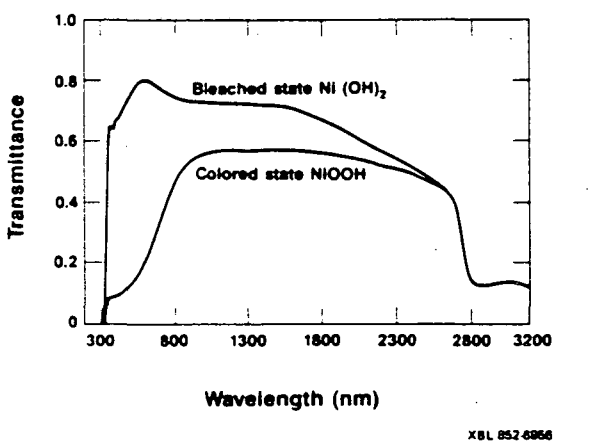

Figure 6b. Normal spectral solar transmittance of electrochromic NiO/SnO_2:F, Cl/glass in bleached and colored states: T_S (bleached) = 0.73, T_S (colored)= 0.35, T_{NIR} (bleached)= 0.72, and T_{NIR} (colored) = 0.55.

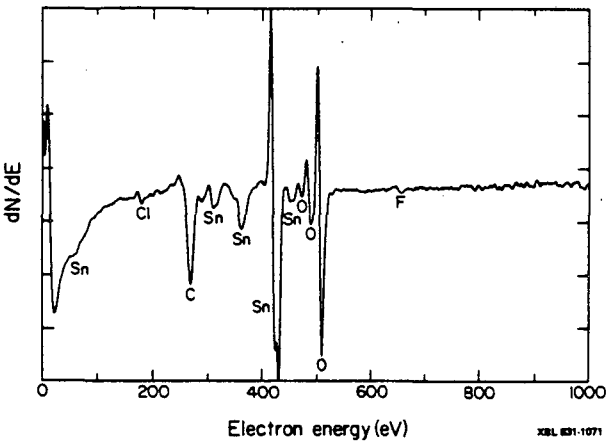

Figure 5b. Auger electron spectroscopy for SnO_2:F, Cl/glass electrode surface.

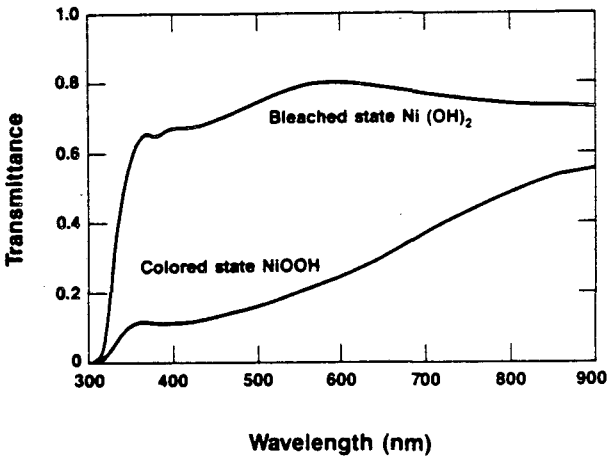

Figure 6a. Normal spectral visible transmittance of electrochromic NiO/SnO_2:F, Cl/glass in bleached and colored states: T_V (bleached) = 0.77 and T_V (colored) = 0.21.

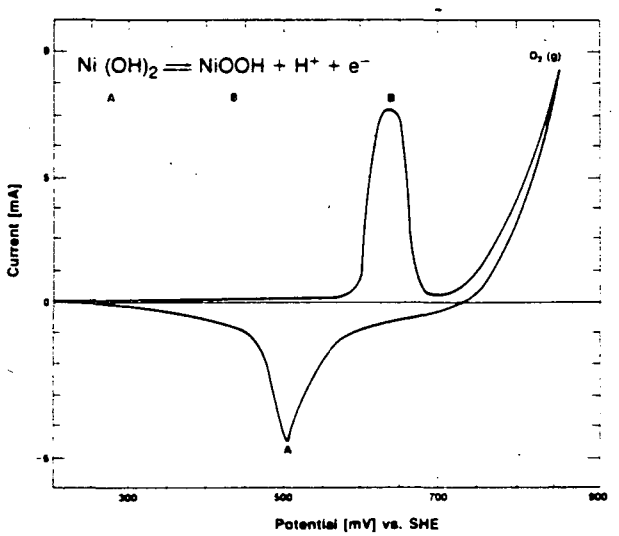

Figure 7. Cyclic voltammetry of NiO/SnO_2:F, Cl/glass electrode after twelve cycles.

The separation of the oxygen evolution potential from the coloration (B) and bleaching (A) potentials, which is evident for nickel oxide, is an important factor in the production of a practical solid-state optical switching device based on proton transfer. Furthermore, for coloration and bleaching of the electrode, only an instantaneous pulse of current is required for the reversible transformation.

Auger spectroscopy and x-ray photoelectron spectroscopy (XPS, ESCA) were used to obtain chemical information about the electrode in the bleached (dehydrated) condition. A chemical depth profile for oxygen and nickel was obtained by sequential argon-ion sputtering and Auger electron analysis. These results are shown in Figure 3. A full survey analysis is given for different depths into the film as shown in Figure 4a-c. Three general regions are noted in the oxide: (1) a surface layer containing a high concentration of oxygen and impurities (Figure 4a), (2) a nickel oxide region (Figure 4b), and (3) a graded nickel-nickel oxide interface (Figure 4c). The principle electronic transitions are Ni_{MNN} = 61, 102 eV, Ni_{KLL} = 716, 783, 848, and 865 eV, and O_{KLL} = 468, 483, and 503 eV. Impurities were identified as S_{LMM} = 152 eV, Cl_{LMM} = 181 eV, C_{KLL} = 272 eV, N_{KLL} = 379 eV, Fe_{MNN} = 47 eV, Fe_{LMM} = 598, 651, and 703 eV, and Na_{KLL} = 990 eV (15). All of the impurities can be attributed to either bath chemistry additions or intrinsic chemical impurities. These impurities probably account for the shoulder noted after the first anodic peak (B) shown in Figure 2. Because the results of the nickel oxide/nickel electrode experiments were promising in terms of electrochromic switching, research was continued on transparent electrodes.

Transparent Tin Oxide Electrode Study

Nickel oxide films were deposited onto doped tin-oxide coated glass electrodes. Since doped tin oxide was used in place of metallic nickel, it was important to characterize this material. Using sputter Auger techniques, a chemical analysis of this electrode was made. The sputter depth profile is shown in Figure 5a. It was taken at a sputter rate of about 400 Å/min. The Auger elemental survey for an as-received condition is depicted in Figure 5b. From these results, the principle composition was determined to be SnO_2:F, Cl. The Auger transitions were C_{KLL} = 272 eV, Cl_{LMM} = 181 eV, Sn_{MNN} = 316, 367, 430, and 437 eV, O_{KLL} = 468, 483, and 503 eV, and Fe_{KLL} = 647 eV, which correspond to standard data (15). By x-ray photoelectron spectroscopy, the binding state of tin in tin oxide was determined. These results are shown in Figure 5c. The positions of the tin binding energies are Sn $3d_{3/2}$ = 494.8 eV and Sn $3d_{5/2}$ = 486.3 eV. Standard reference data show that for SnO_2 the binding energies are Sn $3d_{3/2}$ = 494.9 eV and Sn $3d_{5/2}$ = 486.4 eV (16). Therefore by combined analysis, the conductive oxide is SnO_2:F, Cl.

After electrochemical deposition of nickel oxide on the tin oxide substrate, solar and visible transmittances were measured using a spectrophotometer. Coloration was obtained by applying a one-volt pulse potential at 0.1 Hz. The film was removed from the electrolyte and then rinsed in distilled water without effecting coloration. Optical spectra are shown in Figures 6a and 6b for the visible and solar regions, respectively. By integration with respect to the solar (AM2) (17) and photopic spectra (human eye visible response) (18), the following values were obtained for photopic transmittance and solar transmittance: T_P (bleached) = 0.77, T_P (colored) = 0.21, T_S (bleached) = 0.73, and T_S (colored) = 0.35. If the solar near-infrared is integrated separately (AM2), the values are T_{NIR} (bleached) = 0.72 and T_{NIR} (colored) = 0.55. Also, the properties of the substrate coated with tin oxide were measured; they are T_S = 0.74, T_P = 0.80, and T_{NIR} = 0.71. Therefore in the bleached state, the nickel oxide only slightly alters the optical properties of the tin oxide-coated glass electrode.

Voltammetry was performed on the nickel oxide/tin oxide electrode under the same conditions as for the metal electrode. As depicted in Figure 7, the anodic peak occurs at 630 mV and the cathodic peak occurs at 500 mV. Oxygen evolution occurs at about 750 mV. This voltammogram is very similar to that noted for the oxidized nickel electrode and lacks the anodic shoulder, thought to be caused by impurities.

Chemical analysis of the electrode was determined by Auger spectroscopy and x-ray photoelectron spectroscopy. An Auger depth profile is shown in Figure 8a. Here again near the surface is a highly oxidized impurity region. This is followed by the nickel oxide region and the interfacial region between nickel oxide and tin oxide. A survey Auger scan after 15 seconds of sputtering is shown in Figure 8b. This survey details the nickel impurities to be chlorine, carbon, and nitrogen. Argon was implanted from the sputter beam. To further probe the nickel oxide chemistry, x-ray photoelectron spectroscopy was employed. From this study, the binding energy of the adventitious carbon 1s electron was noted at 284.7 eV. During calibration, adventitious carbon 1s occurred at 284.4 eV, so sample charging amounts to the energy difference. The shape and position of the nickel and oxygen peaks are depicted in Figures 9 and 10, respectively. Comparitive binding energies are shown in Table 1. This data correlates well to known energies for NiO by other investigators (19-22), but there have been some nickel electrode studies that indicate further complexity for this reaction (23, 24). The nickel hydroxides all form a layered structure where there are alternate layers of nickel and hydroxide ions. There exist two phases, α and β for $Ni(OH)_2$, and β and γ for NiOOH. These phases play an important role in the electrode reaction and quite probably in the electrochromic insertion of OH^- or injection of H^+.

Table I. XPS Binding Energies for NiO and Ni Compounds*

Material	$Ni2p_{3/2}$ (eV)	Satellite	$Ni2p_{1/2}$ (eV)	Satellite	O_{1s} (eV)	Ref.
This work	854.7	860.7	872.7	878.7	530.5	—
NiO	854.3	861.5	—	—	529.7	19
NiO	854.4	—	—	—	529.5	20
NiO	855.0	861.1	873.0	879.8	—	21
$Ni(OH)_2$	856.4	862.2	—	—	531.5	19
$Ni(OH)_2$	855.7	—	—	—	531.2	22
Ni	852.3	—	—	—	869.7	16

*All data adjusted for charging and differences in calibration.

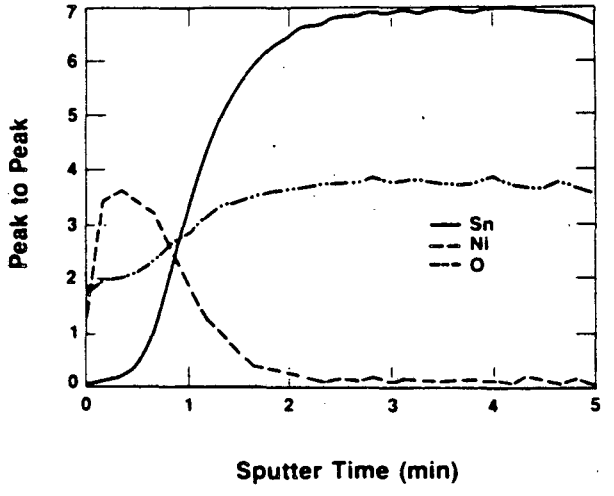

Figure 8a. Auger sputter depth profile of NiO/SnO_2:F, Cl/glass electrode of its peak to peak intensities (sputter rate in Ta_2O_5 = 1000 A/min).

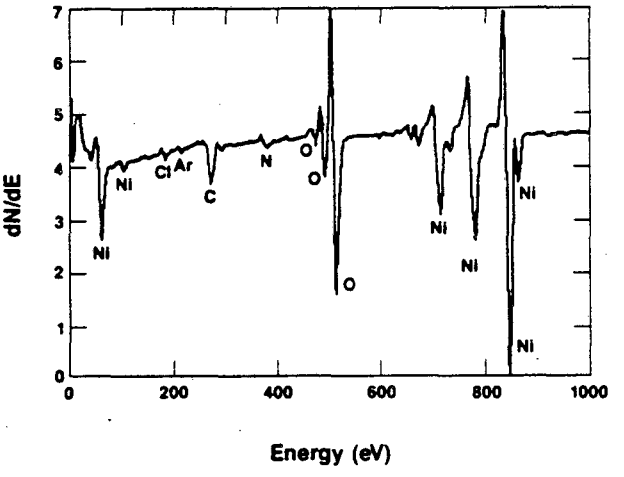

Figure 8b. Auger survey of NiO/ SnO_2:F, Cl/glass electrode.

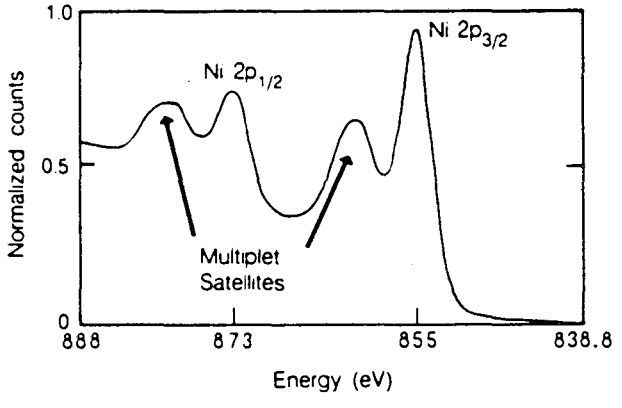

Figure 9. X-ray photoelectron spectroscopy of nickel 2p electrons in NiO, showing the characteristic binding energies.

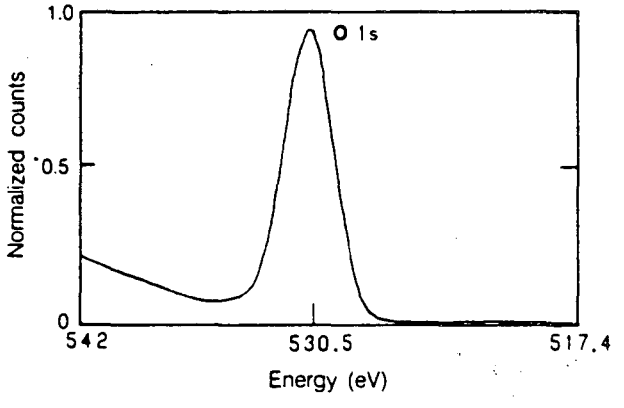

Figure 10. X-ray photoelectron spectroscopy of oxygen is electron in NiO, showing the characteristic binding energy.

Conclusion

As a result of these combined studies, it has been determined that nickel oxide can exhibit favorable electrochromic switching properties for possible use for window glazings. By electrochemical techniques, nickel oxide can be grown on nickel electrodes or deposited onto a conductive oxide such as SnO_2: F, Cl on glass. The optical properties of a 500 A NiO/ SnO_2:F, Cl/ glass electrode were T_p (bleached) = 0.77 and T_p (colored) = 0.21, and T_s (bleached)= 0.73 and T_s (colored) = 0.35. The electrochemical properties of both types of electrodes were determined by cyclic voltammetry. For both the metal and transparent electrode, the voltammetry showed the electrochromic switching reaction to be $Ni(OH)_2 \longleftrightarrow NiOOH + H^+ + e^-$. The chemistry of the electrodes has been determined to be a hydrated form of NiO. Further research is clearly necessary, especially with regard to nickel oxide/ hydroxide films on transparent electrodes, which have not been studied in detail prior to this work. Continued studies utilizing electron microscopy and infrared spectroscopy is planned, in order to determine the exact phases of nickel oxide/ hydroxide films.

Acknowledgments

The authors wish to thank Dr. B. Beard, K. Gaugler, and Dr. S. Cogan (EIC Labs, Norwood, Mass.) for their help with ESCA analysis, scanning Auger microprobe, and electrochemistry, respectively. A special thanks goes to Steve Selkowitz, Prof. J. Washburn, and Dr. T. Sands (Bell Corporate Research Labs, Murray Hill, N.J.), for supporting this effort. This work was performed at the Lawrence Berkeley Laboratory, Materials and Molecular Research Division, under a joint program with the Applied Science Division. The work was funded by the Assistant Secretary for Conservation and Renewable Energy, Office of Solar Heat Technologies, Passive and Hybrid Solar Energy Division of the Department of Energy under Contract No. DE-AC03-76SF00098.

References

1. Lampert, C. M., "Electrochromic Materials and Devices for Energy Efficient Windows," Solar Energy Materials, Vol. 11, p.1, 1982.

2. Dautremont-Smith, W.C., "Transition Metal Oxide Electrochromic Material and Displays: A Review," Displays, Vol. 4, p.3, 1982.

3. Chang, I. F., in Nonemissive Electrooptic Displays, Kmetz, A.R., and Von Willisen, F. K., edit., Plenum, New York, 1976.

4. Fangham, B.W., and Crandall, R. S., in Topics in Applied Physics, Vol. 40, Pankove, J. I., edit., Springer-Verlag, Berlin, 1980.

5. McIntyre, J. D., Peak W. F., and Schwartz, G. P., "Electrochromism in Hydrous Nickel Oxide Films," Electronic Materials Conference Abstract, D-4, 1979.

6. Goldner, R. B., et al., "High Near Infrared Reflectivity Modulation with Polycrystalline Electrochromic WO3," Applied Physics Letters, Vol.43, p. 1093, 1983.

7. Vashistita, P., Mundy, J. N. ,and Shency, G. K., Fast Ion Transport in Solids, North-Holland, Amsterdam, The Netherlands, 1979.

8. Lampert, C. M., "Materials Chemistry and Optical Properties of Transparent Conductive Thin Films for Solar Energy Utilization," Ind. Eng. Chem. Prod. Res. Dev., Vol. 21, p. 612, 1982.

9. Schrebler-Guzman, R. S., Vilche, J. R., and Arvia, A. J., "The Potentiodynamic Behavior of Nickel in Potassium Hydroxide Solutions," J. Appl. Electrochem., Vol.8, p. 67, 1978.

10. Weininger, J. L., and Breiter, M. W., "Effect of Crystal Structure on Anodic Oxidation of Nickel," J. Electrochem. Soc., Vol. 110, p. 484, 1963.

11. Weininger, J. L., and Breiter, M. W., "Hydrogen Evolution and Surface Oxidation of Nickel Electrodes in Alkaline Solutions," J. Electrochem. Soc., Vol. 111, p. 707, 1964.

12. MacArthur, D.M., "The Hydrated Nickel Hydroxide Electrode Potential Sweep Experiments," J. Electrochem Soc., Vol.117, p. 422, 1970.

13. Briggs, G. W. D., and Fleischmann, M., Trans. Faraday Soc., Vol. 67, p. 2397, 1971.

14. Schrebler-Guzman, R. S., Vilche, J. R., and Arvia, A. J.,"The Kinetics and Mechanism of the Nickel ElectrodeIII, The Potentiodynamic Response of Nickel Electrodes in Alkaline Solutions in the Potential Region of Ni(OH)2 Formation," Corrosion Science, Vol. 18, p. 765, 1977.

15. Handbook of Auger Electron Spectroscopy, Physical Electronics Industries, Eden Prairie, MN., 1976.

16. Wagner, C. D., Riggs, W. M., Davis, L. E., and Moulder, J. F., Handbook of X-Ray Photoelectron Spectroscopy, Physical Electronics Industries, Eden Prairie, MN., 1979.

17. Bird, R. E., and Hulstrom, R. L. "Additional Solar Spectral Data," Solar Cells, Vol. 8, p. 85, 1983.

18. Barnes, F. A., edit., RCA Electro-Optics Handbook, RCA Corporation, Harrison, N J., 1974.

19. Kim, K. S., Baitinger, W. E., Amy, J. W., and Winograd, N., "ESCA Studies of Metal-Oxygen Surfaces using Argon and Oxygen Ion Bombardment," J. Elect. Spect. and Rel. Phenom., Vol. 5, p. 351, 1974.

20. Kim, K. S., and Davis, R. E., "Electron Spectroscopy of the Nickel-Oxygen System," J. Elect. Spect. and Rel. Phenom., Vol. 1, p. 251, 1972/73.

21. Matienzo, L. J., Yin, Lo. I., Grim, S. D., and Swartz, Jr., W. E.," X-Ray Photoelectron Spectroscopy of Nickel Compounds," Inorg. Chem., Vol. 12, p. 2762, 1973.

22. McIntyre, N. S., Rummery, T. E., Cook, M. G., and Owen, D., "X-Ray Photoelectron Spectroscopic Study of the Aqueous Oxidation of Monel 400," J. Electrochem Soc., Vol. 123, p. 1164, 1976.

23. Bode, H., Dehmelt, K., and Nitte, J. "Zur Kenntnis der Nickelhydroxidelelektrode- I Uber das Nickel (II) Hydroxidhydrat," Electrochim Acta., Vol. 11, p. 1074, 1966.

24. Oliva, P., et al., "Review of the Structure and the Electrochemistry of Nickel Hydroxides and Oxy-Hydroxides," J. Power Sources., Vol.8, p. 229, 1982.

LAWRENCE BERKELEY LABORATORY
TECHNICAL INFORMATION DEPARTMENT
UNIVERSITY OF CALIFORNIA
BERKELEY, CALIFORNIA 94720